Title

Successive passaging of a plant-associated microbiome reveals robust habitat and host genotype-dependent selection

Journal

Proceedings of the National Academy of Sciences of the United States of America, 117(2)

ISSN

0027-8424

Authors

Morella, Norma M
Weng, Francis Cheng-Hsuan
Joubert, Pierre M
et al.

Publication Date

2020-01-14

DOI

10.1073/pnas.1908600116

Peer reviewed

Title

Successive passaging of a plant-associated microbiome reveals robust habitat and host genotype-dependent selection

Authors

Morella, Norma M.[1*], Weng, Francis Cheng-Hsuan[3], Joubert, Pierre M.[1], Metcalf, C. Jessica E. [4], Lindow, Steven[1], Koskella, Britt[2*]

Author affiliations

1 Department of Plant and Microbial Biology, UC Berkeley, Berkeley, CA, USA

2 Department of Integrative Biology, UC Berkeley, Berkeley, CA, USA

3 Biodiversity Research Center, Academia Sinica, Taipei, Taiwan

4 Department Ecology, Evolutionary Biology & Public Affairs, Princeton University, Princeton, NJ, USA

* To whom correspondences should be addressed

Abstract

There is increasing interest in the plant microbiome as it relates to both plant health and agricultural sustainability. One key unanswered question is whether we can select for a plant microbiome that is robust after colonization of target hosts. We used a successive passaging experiment to address this question by selecting upon the tomato phyllosphere microbiome. Beginning with a diverse microbial community generated from field-grown tomato plants, we inoculated replicate plants across five plant genotypes for four eight-week long passages, sequencing the microbial community at each passage. We observed consistent shifts in both the bacterial (16S amplicon sequencing) and fungal (ITS amplicon sequencing) communities across replicate lines over time, as well as a general loss of diversity over the course of the experiment, suggesting that much of the naturally observed microbial community in the phyllosphere is likely transient or poorly adapted within the experimental setting. We found that both host genotype and environment shape microbial composition, but the relative importance of genotype declines through time. Furthermore, using a community coalescence experiment, we found that the bacterial community from the end of the experiment was robust to invasion by the starting bacterial community. These results highlight that selecting for a stable microbiome that is well adapted to a particular host environment is indeed possible, emphasizing the great potential of this approach in

agriculture and beyond. In light of the consistent response of the microbiome to selection in the absence of reciprocal host-evolution (co-evolution) described here, future studies should address how such adaptation influences host health.

Keywords

Microbiome assembly; microbiome selection; microbiome engineering; experimental evolution; phyllosphere; Solanum

Significance Statement

There is great interest in selecting for host-associated microbiomes that confer particular functions to their host, and yet it remains unknown whether selection for a robust and stable microbiome is possible. Here, we use a microbiome passaging approach to measure the impact of host-mediated selection on the tomato phyllosphere (above ground plant surfaces) microbiome. We find robust community responses to selection across replicate lines that are shaped by plant host genotype in early passages, but are genotype-independent in later passages. Work such as ours is crucial to understanding the general principles governing microbiome assembly and adaptation, and is widely applicable to both sustainable agriculture and microbiome-related medicine.

Introduction

The study of microbiomes (diverse microbial communities and their collective genomes) spans both basic and applied research in human health, agriculture, and environmental change. As our understanding of the ability of the microbiome to influence host health and shape host traits deepens, there is increasing interest in selecting and/or designing microbiomes for specific traits or functions. Such trait-based selection of microbiomes has the potential to shape the future of agriculture and medicine [1–3]. In agriculture, below-ground microbiota have already proven capable of shifting the flowering time of plant hosts [4], enhancing drought resistance [5, 6], improving plant fitness [7], and even altering above-ground herbivory [8]. However, long-term, repeatable success of future efforts will rely on a fundamental understanding of the assembly of, selection within, and co-evolution among microbiota within these communities. One of the challenges facing successful, rational microbiome manipulation and assembly is disentangling the forces naturally shaping the communities, including both host characteristics and microbial immigration on community stability. For example, in both humans and plants, there is conflicting evidence as to the relative importance of the environment versus host genotype in shaping the microbiome [9–17], and dispersal has been shown to override host genetics in an experimental zebra fish system [18].

One powerful but under-utilized approach to understand and experimentally control for the factors shaping microbiome composition and

diversity is experimental evolution. Measuring changes of populations or communities over time under controlled settings in response to a known selection pressure has proved a powerful force in gaining fundamental understanding of both host-pathogen (co)evolution [19] and microbial evolution [20]. Here, we harness an experimental evolution approach in order to study how an entire microbial community can be selected upon in a plant host environment that varies across disease resistance-associated genotypes. We test the fundamental yet relatively untested assumption that a microbiome can be selected to adapt to its host in a robust fashion. We do so in the absence of selection on a particular plant-associated trait (e.g. flowering time or fecundity) in an attempt to capture how an entire community might naturally change over time to become well adapted to a host environment. To do this, we employ a microbiome passaging approach using the phyllosphere microbiome of tomato (*Solanum*) as a model system to select for a community that is capable of growth in this relatively oligotrophic environment and is resilient to perturbation via competition with a non-‘adapted,’ but more diverse community. The phyllosphere, defined as the aerial surfaces of the plant, is a globally important microbial habitat [21], and can shape important plant traits such as protection against foliar disease [22, 23] and growth [24, 25]. Successful trait-based selection on the phyllosphere (previously undemonstrated) could therefore allow for enhancement of plant health, but this critically depends on the ability to select for a well-adapted microbial community that is relatively stable

against invasion, particularly in open environments in which dispersal from neighboring hosts or the surrounding environment is inevitable.

We collected a diverse phyllosphere microbiome from tomatoes grown in an agricultural setting and transplanted it onto green-house grown plants using a transplantation method previously shown to be effective for lettuce [26]. We serially passaged this diverse microbiome on each of four cohorts of tomato plants (six lines per cohort) of five different genotypes (pairs of near isogenic *S. lycopersicum* genotypes that differed at known disease resistance loci, as well as a wild tomato accession, *S. pimpinellifolium*) for a total of 30 weeks. On each plant, during each passage, community assembly and dynamics might be driven by neutral processes or reflect positive or negative selection of specific taxa by the plant, dispersal of taxa from the greenhouse environment, and/or the other microbial taxa present. We therefore sought to characterize the relative importance of neutral versus deterministic processes both computationally using a neutral model, and empirically using community coalescence experiments [27] in which communities from different passaged lines are combined together and re-inoculated onto host plants in a common garden experiment. Overall, we were able to measure and characterize the response of the phyllosphere microbiome to selection in the plant host environment under greenhouse conditions, and our findings suggest selection for a stable and well-adapted plant-associated microbiome.

Results

Serial passaging experiment

A diverse starting inoculum was collected from field grown, mature tomato plants. This field-microbiome was spray inoculated onto 30 tomato plants of 5 different genotypes, with six replicates each (Figure 1a). Two-week old tomato plants were spray-inoculated once per week for five weeks, and then sampled in their entirety ten days after the final inoculation (Figure 1b). The phyllosphere microbiome of each plant was then individually passaged on these genetically distinct hosts over the course of four eight-week long passages; P1, P2, P3, and P4 (Figure 1a; see methods for details). Microbiomes were not pooled across plants within a given plant genotype, resulting in 30 independent selection lines. Control plants were inoculated with an equal volume of either heat killed inoculum (P1) or sterile buffer (subsequent passages) every week. At the end of each passage, bacterial density was measured and normalized to the weight of each plant (Figure 1c), and communities were sequenced using 16S rRNA amplicon sequencing.

We first measured the impact of host genotype on bacterial community structure (Figure 2a). Using Bray-Curtis dissimilarity measures, we performed permutational multivariate analysis of variance tests (PERMANOVA) at each passage using the Adonis function in the Vegan R package [28, 29]. We found that in P1, plant genotype explains 29% of dissimilarity between microbiomes ($F_{4, 27} = 2.331$, $p = 0.003$). This result is

robust to the removal of an outlying sample (see supplement for statistical results of that model). In P2, plant genotype similarly explains 28% of the variation in bacterial community dissimilarity ($F_{4, 24}$ =1.906, p=0.004). However, genotype becomes an insignificant driver of community composition in both P3 (R^2=0.18, $F_{4, 23}$= 1.018, p=0.378) and P4 (R^2=0.09, $F_{3, 19}$= 0.527, p=0.937). The five genotypes can be classified as pathogen "resistant" or "susceptible" based on known loci, and despite the overall effect of genotype at P1 and P2, there was no significant effect of disease resistance on Bray-Curtis dissimilarities either overall or in any single passage. In some passages, an unequal number of samples across genotypes were analyzed due to exclusion of samples with poor sequencing quality. In order to account for this and ensure the genotype effect observed in P1 and P2 was not due to heterogeneous dispersion of samples within a group, we tested for homogeneity of multivariate dispersions using the betadisper function in Vegan [30, 31]. The betadispersion results are insignificant in both P1 (p=0.234) and P2 (p=0.231), indicating that the significant effects of genotype observed above are likely not an artifact of dispersion and indeed reflect biological differences. To further test the robustness of these findings, we removed replicate lines from accession 2934 and re-analyzed the data. We did so because lines from accession 2934 were lost after P3 due to a stem rot fungal pathogen present in the original inoculum that seemingly only infected this genotype. Significance of genotype in all passages is

unchanged by exclusion of these lines from the dataset (see supplement for statistical details).

We next sought to determine if there were more subtle influences of host genotype on the community that were not uncovered through analyzing Bray-Curtis dissimilarity alone. From the original inoculum sample, we identified ten Operational Taxonomic Units (OTUs) using linear discriminant analysis effect-size (LEfSe) [32] that were significantly associated with particular genotypes in P1 and P2. We compared their presence/absence at the end of P4 to those OTUs that were not found to be associated with genotype. Interestingly, those OTUs that were significantly associated with particular genotypes at the start of the experiment were significantly more likely to be present at the end of the experiment than those not associated with genotype (Fisher's exact test, p=0.013), suggesting that the loss of genotype effect observed was not driven by loss of particular genotype-associated OTUs.

In addition to genotype effects, we were interested in what other factors were driving the observed change in community composition. Using a multivariate PERMANOVA, we found that the both the number of passages on tomato plants and sample type (e.g. experimental, control, or inoculum) strongly shaped microbial community diversity (Supplementary Figure S1: Passage: R^2=0.408, $F_{3, 110}$= 27.764, p= 0.001; Sample Type: R^2=0.043, $F_{5, 110}$= 4.379, p= 0.001). Again, we find the results of a betadispersion test are insignificant for both passage and sample type,

indicating that the observed significant effects are likely not an artifact of unequal dispersion (Passage: $F_{3,112}$= 1.501, p=0.201; Sample Type: $F_{2,113}$= 1.457, p=0 0.213). When inoculum and control samples are removed from analysis, there remains both a significant effect of passage number and an overall effect of plant genotype (Passage: R^2= 0.514, $F_{3, 89}$= 34.191, p=0.001; Genotype: R^2=0.040, $F_{4, 89}$= 1.999, p=0.001). In this model, we took into account that individual microbiome lines were passaged and sampled at each passage by performing the multivariate PERMANOVA with Line ID used as strata. Note: we were unable to conduct a true nested time-series analysis with our multivariate data due to limitations of currently available statistical tests (see methods for specific models and further discussion). As above, we performed a betadispersion test and found no significant effect of dispersion regarding genotype or passage (Genotype: $F_{4, 92}$= 0.725, p= 0.58; Passage: $F_{3, 93}$= 2.359, p= 0.077). Taken together, the results of these models indicate that the reported findings are robust to differences arising due to both repeated sampling of the same lines and unequal sample sizes between genotypes and passages.

We next sought to determine the role of dispersal of taxa amongst tomato plants on the greenhouse bench in shaping the phyllosphere microbiome over time. We did this by directly comparing the communities found on experimental and control plants. We calculated the proportion of OTUs on control plants that were from the inoculum that was sprayed onto experimental plants. At every passage, over 50% of inoculum OTUs were

231 detectable on control plants, suggesting that dispersal in the greenhouse
232 was occurring. Despite this, control and experimental plants are found to
233 host significantly different communities at every passage (PERMANOVA: all
234 p-values <0.04) and overall have significantly lower bacterial abundance
235 (Figure 1c). Taken together, these data suggest that the effects of low
236 levels of dispersal of taxa amongst plants in the experiment (as might be
237 expected due to the plants' proximity to one another and their
238 randomization on the greenhouse bench) are minimal relative to the
239 effects resulting from inoculations.
240 To better understand how the original, diverse, field inoculum
241 changed over four passages on plants in the greenhouse, we calculated the
242 percentage of OTUs in the original inoculum that were detectable over the
243 course of the experiment (Figure 2b, green diamonds). At the end of P1,
244 92% of the field inoculum OTUs were still present on the plants, but by P4,
245 this was reduced to 29%. We then calculated if the decrease in original
246 community member diversity was the result of replacement by non-
247 inoculum taxa (i.e. those that colonized plants over the course of the
248 experiment). In this case, we observed that the proportion of sequencing
249 reads (divided by total reads) representing the original inoculum OTUs
250 remains above 78% (Figure 2b, box plots). This indicates poor persistence
251 of the majority of the original taxa from the field-grown plant inoculum, but
252 those that remained seemed to dominate the community. This also
253 suggests that a relatively small percentage of the community was made up

of OTUs that colonized plants from the greenhouse environment. Furthermore, there is no visual indication (heat map presented in Supplemental Figure S2) that a large portion of these non-inoculum OTUs arrived and persisted on the plants for multiple passages. Of note, some OTUs considered "non-inoculum" were likely present in the initial inoculum, but in too low of abundance to detect. To account for the impact of the small percentage of arriving species on community composition, we re-analyzed the dataset using only those OTUs that were observed to be present in the initial inoculum (Supplemental Figure S3a). Using the same multivariate PERMANOVA models as above with permutations limited to within Line IDs, we found that passage number and genotype remain significant drivers of community dissimilarity (Passage: R^2= 0.546, $F_{3, 87}$= 38.192, p=0.001; Genotype: R^2= 0.039, $F_{4, 87}$= 2.062, p=0.001).

We next measured changes in bacterial density and diversity over the course of passaging and across lines. In P1, we estimated the fold change of bacterial abundance on control plants that were sprayed with heat-killed inoculum, and found an average change of 0.76, which is significantly lower than the averaged 11-fold change for experimental plants which received live inoculum (Welch's Two sample T-Test, p<0.0001). Using a repeated measures ANOVA, we found an overall significant decrease in both OTU richness and alpha diversity over time across all plant genotypes (p<0.001 for both). Significant differences between each passage were determined by multiple comparisons of

means, and corrected P values (using Bonferroni corrections) are illustrated on Figure 2c-d and Supplemental Figure S3b. Neither genotype nor overall disease resistance had a significant effect on richness and diversity at any passage. Importantly, the overall drop in diversity from P1 to P4 does not correspond to a decrease in overall bacterial abundance on plants (see Figure 1c). To test whether this decrease in richness and diversity could be driven by replacement of slower-growing taxa with fast-growing competitors, we analyzed 16S rRNA mean copy number as an indicator of bacterial ecological strategies [33–35]. At each passage, we analyzed taxa that made up 95% of total reads. For each taxon, we recorded mean 16S copy number for that particular family using the rrnDB [36] and calculated "copy number to relative abundance" ratio for each taxon at each passage (1 through 4). We found that there is no significant effect of Passage on "copy number to relative abundance" ratio (ANOVA: $F_{3, 54}$=0.735, p=0.536). There is also not a significant effect of Passage on "copy number" (where copy number is not normalized to relative abundance of that taxon; $F_{3, 54}$=0.738, p=0.534). Finally, although passaging was performed in a control temperature greenhouse, outside high and low temperatures and humidity all varied significantly across passages (Supplemental Figure S4; ANOVA P<0.001 for all measures), which may have impacted the observed differences in both abundance and growth across passages.

With the knowledge that communities were drastically changing over

time, we sought to determine if the rate at which the communities were changing was consistent. To do this, we calculated Bray-Curtis dissimilarity of microbiomes in each passage to P1 microbiomes (Figure 2e). As we similarly observed through ordination plots in Figure 1, the communities become more dissimilar to P1 over time. We then fit both a linear and quadratic regression to these data, and we found that both were significant, but there is a better fit of a quadratic model than linear as evidenced by higher R^2 and lower AIC values (Linear R^2 0.774, AIC -3563.231; Quadratic R^2 0.8379, AIC: -4414.637). When the regression models are compared using an ANOVA, we find that the quadratic model is a significantly better fit for the data ($p<0.0001$), suggesting that the rate of community change may be slowing down. However, when we calculate Bray-Curtis dissimilarity across passages for each microbiome line, we observe no significant effect of "passage comparison" on Bray-Curtis dissimilarity (Supplemental Figure S5; ANOVA: $F_{1, 17}= 0.332$, $p= 0.572$), suggesting that the community change may be slowing with respect to comparison to P1, but rate of change from one passage to another seems more constant. From the same model, we also find a moderately significant effect of "Line ID" on dissimilarity, indicating that some lines may be have changed at a different rate than others ($F_{26, 17}= 1.396$, $p= 0.052$). We did not find there to be a significant interaction between LineID and Comparison ($F_{20, 17}= 1.396$, $p=0.246$).

We next observed changes in relative abundance of specific taxa

within lines over time (Figure 3, top 100 OTUs plotted). At each passage, there are numerous taxa that are differentially abundant compared to other passages. In some cases, there was evidence for replacement of OTUs within taxonomic groups. For example, within the family *Pseudomonadaceae*, there are three OTUs that are differentially abundant between P1 and P4.

Two *Pseudomonads* (OTU0010 and 0004) are in significantly higher relative abundance in P1 compared to P4 (paired samples Wilcoxon test: $p<0.0001$). As visualized in Figure 3, these taxa gradually decrease in relative abundance over the course of passaging. An unclassified *Pseudomonadaceae* (0002) is significantly more abundant in P4 as compared to P1 (paired samples Wilcoxon test: $p<0.0001$). All three OTUs are present in the initial spray inoculum, although OTU0002 represents only 0.03% of rarified spray inoculum reads whereas *Pseudomonas* OTU0004 represents 27% and *Pseudomonas* OTU0010 represents 21%.

To better understand how bacterial community dynamics were changing over the course of the four passages, we utilized a recently developed cohesion metric to quantify connectivity of a microbial community [37]. In brief, community cohesion is a computational method used to predict within-microbiome dynamics by quantifying connectivity of microbial communities based on pairwise correlations and relative abundance of taxa. Changes in community cohesion over time are suggestive of biotic interactions, where connectivity can arise from either,

or both, positive and negative interactions resulting from cross-feeding (positive) or competition (negative) as well as environmental co-filtering. When applied to our dataset (Supplemental Figure S6a), we find a minor but significant increase in positive cohesion values (among 200 permutations) from P1 to P4 (R^2=0.19, p<0.0001). Consistent with positive cohesion values showing increased biotic interactions, there are also increasingly negative cohesion values from P1 to P4, which again is minor but significant (R^2=0.257, p<0.0001). To further test our hypothesis that community change was due to deterministic processes, a null prediction was generated based on the known community composition of inocula applied at each passage, and we compared our observed communities to the predicted neutral community using a recently developed approached [38] (see methods for complete details). We found that Bray Curtis dissimilarities between predicted (null) and observed communities moderately increases over time (R^2=0.261, p<0.0001; Supplemental Figure S6b), as would be expected if community change over the course of the experiment is the result of deterministic rather than stochastic processes.

Further evidence for a shift away from neutrality can be observed using occupancy- abundance curves in which the occupancy, or proportion of individuals in which an OTU is found, is plotted against its relative abundance (Figure 4). A positive correlation between the two is expected to occur by chance, as observed in a neutrally assembled community, but a change in distribution of individuals may indicate a community shaped by deterministic

processes [39, 40]. When our data are visualized in this manner, we see that in P1 (Figure 4a), the most abundant taxa also occupy the highest proportion of plants, as you would expect in a neutral community not undergoing niche selection. However, this trend collapses by P4 (Figure 4d) with many abundant taxa occupying far fewer individuals than would be expected under neutrality. When regressions are fit to these distributions, there is an overall decrease in correlation between occupancy and abundance, regardless of whether a linear or polynomial regression is used. Fit to a linear model decreases from an R^2 of 0.88 at P1 to 0.60 at P4. There is a significant effect of Phyla on the linear model fit across all passages (ANOVA: $F_{4, 12} = 5.318$, p= 0.0107). Overall, a polynomial (n=4) regression is a better fit to the data (P1: R^2=0.96; P4: R^2=0.66), but the effect of Phyla in this case is insignificant (ANOVA: $F_{4, 12} = 2.566$, p= 0.0924).

We next designed an experiment in which we could explicitly test the robustness of the shift away from neutrality by comparing empirical results to model predictions. The experimental design (Supplemental S7a) was to pool together all lines from the end of P4 and re-inoculate this single inoculum onto replicate tomato plants across genotypes, mimicking the inoculation procedure from the first passage and allowing for a direct comparison to neutral models assuming a shared species pool. Plants that received the P4-combined inoculum had significantly different bacterial community composition than the P4 plants themselves (48% of variation explained, P=0.001; Supplemental S7b). Unlike in P1, we did not observe

an effect of genotype on the communities assembled from this combined inoculum (p=0.565). We also found that the majority of the variation between samples (76%, p=0.001) was driven by an exceptional situation of introduction of a greenhouse taxon (OTU0003) to the plants (Supplemental S7c). To test if neutral processes were driving community structure in this experiment, we applied the Sloan neutral community model [41] to our data. This model assumes equal dispersal amongst hosts (and thus it could not be used for analysis of P2-P4 data, as microbiomes were passaged without pooling.) In this case, as with P1, the assumption of equal dispersal potential among plants is met. In 200 iterative predictions, the fit of the neutral model is significantly higher in P1 (R^2=0.87 ± 0.01) than P4-Combined (R^2=0.52 ± 0.05; Student's *t*-test, *p*-value < 0.01), suggesting that neutral processes are dictating the community structure after the first passage, but not in the P4-Combined experiment (Supplemental S7d). We also see the occupancy-abundance relationship breakdown in P4-Combined when compared to P1 directly (Supplemental S7e).

Mycobiome

In an effort to understand how the fungal community changed overall from the first to the final passage, we used ITS amplicon sequencing to describe the fungal communities across lines in P1 and P4. We observe patterns that are similar in some regards to the bacterial communities. Using multivariate PERMANOVA models as were performed for the bacterial

dataset, we again found both a significant effect of passage number and sample type on fungal communities (Supplemental Figure S8a; Passage: R^2= 0.42, $F_{1, 43}$= 34.3948, p=0.001; Sample Type: R^2= 0.048, $F_{2, 43}$= 1.976, p= 0.043). The significant effect of passage number remained after inoculum, control samples, and accession 2934 were removed and LineID were used as strata for permutations (Supplemental Figure S8b; R^2= 0.472, $F_{1, 38}$= 34.021, p=0.001). However, unlike in the bacterial community analysis, we found no significant differences in community composition between control and experimental plants when this was tested at each passage using a series of univariate PERMANOVAs (P1 $F_{1, 21}$= 2.1057, R^2= 0.09113, p=0.066; P4 ($F_{1, 24}$=0.6479, R^2= 0.02629, p=0.612). Additionally, we did not find an effect of host genotype at either passage ($F_{4, 16}$= 0.87756, R^2= 0.17992, p=0.595; $F_{3, 19}$=0.92402, R^2= 0.12732, p=0.53). We also measured a significant decrease in both OTU richness (paired samples Wilcoxon tests, p=0.0316) and Shannon's diversity (p=0.0067) between P1 and P4 across all genotypes (Supplemental Figure S8c, d). In all analyses, there were no significant effects of disease resistance. Finally, analysis of the five most common taxa overall identified a single OTU, identified as *Rhodosporidiobolus nylandii*, which was not detectable in the inoculum or P1 but which dominated the fungal community in P4 (Supplemental Figure S8e).

Testing microbiome adaptation using community coalescence

The similarity of changes in community structure both across replicates and genotypes over the course of the passaging experiment (Figures 1-4) led us to predict that these microbiomes were becoming well adapted to the local plant conditions (by which we mean that the taxa present were positively selected for over time). To further determine if the community changes we observed from P1 to P4 were due to habitat selection rather than neutral processes, we employed a community coalescence competition experiment. In this experiment (Figure 5a), phyllosphere communities from the end of P1 (pooled across all lines) and the end of P4 (again, pooled across lines) were inoculated onto a new cohort of plants, either on their own or in an approximately 50:50 mixture of live cells (as determined using live/dead PMA treatment followed by ddPCR; see methods for complete details). To ensure that our method for the mixed inoculum was effective, we sequenced multiple replicates of the P1, P4, and Mix inocula and began by comparing just these original inoculum samples. We found that source explains 88% of dissimilarity amongst inocula (PERMANOVA: $F_{2, 8}$= 30.196, p=0.002). A betadispersion test was insignificant, indicating differences in inoculum samples were not due to heterogeneous variance ($F_{2,8}$= 1.536, p= 0.28). To confirm that the Mix inoculum was significantly different than both P1 and P4 separately, we compared P1 and Mix inocula directly and found that 75% of difference between samples can be explained by this variable (PERMANOVA: $F_{1, 5}$= 15.138, p=0.022). Similarly, when P4 and Mix are compared directly, 74%

of variation in the community is explained (PERMANOVA: $F_{1,5}$=13.999, p=0.032). This consistent difference among the starting inocula allowed us to compare the communities colonizing plants from each treatment.

We first measured final bacterial abundance and found that colonization was lower on these plants than in previous experiments, but did not significantly differ among treatments (ANOVA: $F_{3, 32}$= 0.971, p=0.419), apart from control plants, where bacterial colonization was greatly reduced (Figure 5b). We then compared bacterial communities again using 16S amplicon sequencing. Plants that received P1 inoculum have distinctly different communities than those that received either P4 or the Mixed inoculum (Figure 5c). Plants that received the Mixed inoculum clustered together with those receiving P4 and were relatively indistinguishable. Using a multivariate PERMANOVA, we determined that inoculum source can explain 45% of Bray-Curtis dissimilarity amongst samples ($F_{2, 31}$= 13.486, p=0.001), but there was no effect of plant genotype (R^2=0.034, $F_{2, 31}$= 1.017, p= 0.376; although note that only three genotypes were used in this experiment). In a pairwise analysis between P1 and Mixed, inoculum source explains 39% of the community dissimilarity (PERMANOVA: $F_{1, 22}$= 13.988, p=0.001). In contrast, inoculum source does not explain any significant variation in dissimilarity amongst P4 and Mixed inoculum plants (PERMANOVA: $F_{1, 22}$= 2.4378, p=0.103). Together, these results suggest that the plants receiving the 50:50 mixed inoculum were indistinguishable in community composition from those

484 receiving the pooled, P4 passaged microbiomes, and thus that these
485 selected communities were not invadable by the microbial communities
486 from the start of the experiment. Consistent with our results from the
487 passaging experiment itself, alpha diversity was found to be highest in P1
488 plants compared to both P4 and Mixed plants (Figure 5d). Alpha diversity
489 did not differ amongst communities colonizing plants from the P4 and
490 Mixed inoculums, despite being different between the two inocula
491 themselves. We also examined compositional makeup of the communities
492 (Figure 5e), and consistent with P1 to P4 passaging results, we see
493 differentially abundant taxa between groups (Supplemental Figure S9).
494 Again, two *Pseudomonas* OTUs are more abundant in P1 plants as
495 compared to P4 and Mix, in which there is an unclassified *Pseudomonaceae*
496 that is higher in relative abundance.
497
498 **Discussion**
499 The impact of a microbiome on host health and fitness depends not
500 only on which microbial organisms are present in the community, but also
501 on how they interact with one another within the microbiome [42].
502 Unlocking the great potential of microbiome manipulation and pre/probiotic
503 treatment in reshaping host health will therefore depend on our ability to
504 understand and predict these interactions. We took a microbiome
505 passaging approach, inspired by classic experimental evolution, to test
506 how selection for growth in the tomato phyllosphere under greenhouse

conditions would impact microbiome diversity and adaptation across genotypes that differ in disease resistance genes.

Across independently selected lines passaged on five tomato genotypes, we observed a dramatic shift in community structure and composition, accompanied by a loss of alpha diversity (Figures 1 and 2). We cannot differentiate the relative contribution of evolutionary versus ecological change to the communities, but we expect both to have occurred within the time scale of these experiments. We also found that host genotype shapes bacterial community composition early in passaging (P1 and P2), explaining over 24% of variation amongst samples, but diminishes over time. We had originally predicted that disease resistance would impact the microbiome as a whole as a result of differing interactions with the host immune system. Interestingly, however, we did not observe an overall effect of resistance in shaping community composition. This suggests that there were other genetic differences among hosts that were driving the effect of genotype on microbiome composition in P1 and P2. In general, the relative importance of host genotype and environment in shaping microbiome composition remains highly debated. Our results suggest that the relative importance of genotype versus other factors, such as the growth environment or strength of within-microbiome interactions, changes over the course of passaging on a constant host background. It is possible that genotype-driven differences may become subtler after selection, and thus we are unable to detect them by OTU analysis. Future studies taking a more

fine-scale resolution may be able to detect subtler effects when overall taxa richness decreases. We did find that even in the absence of a strong genotype effect, there remains a legacy of genotype effect, in that OTUs found to be significantly associated with particular genotypes early on are more likely to be present at the end of passaging than those that did not exhibit any host preference.

In order to test if the phyllosphere microbiome undergoes habitat filtering, we chose to begin the experiment with a diverse inoculum. This starting community generated from field grown tomato plants likely contained microbes from other surrounding plant species, dust, soil, and other sources. In particular, neighboring plants have been shown to contribute to both the density and composition of local airborne microbes [43]. We found that although the total number of these field inoculum OTUs decreased over the course of the experiment, the taxa that remained consistently made up 78-95% of the community. This provides strong evidence that the original spray inoculum underwent niche selection over the course of the experiment. We also see evidence for niche selection through changing occupancy-abundance distributions. Increased incidents of high-abundance, low-occupancy taxa in P4, or “clumping” [39], is suggestive of niche selection. Gonzalez et al. found a similar breakdown of occupancy-abundance relations in animal communities using miniature moss microcosms [40]. The authors predict that this was due to dispersal limitation, as their experimental design created habitat fragmentation, and

553 they did not observe this similar decline in correlation in communities that
554 were connected by “habitat corridors”.
555 In this work, we detect some evidence for dispersal both amongst
556 plants and from the environment onto the plants. Specifically, we
557 consistently find OTUs on control plants that originated from the spray
558 inoculum that experimental plants received, indicating that some taxa were
559 spread amongst all plants via, for example, water splash, touching leaves, or
560 insects. We also find a continual influx of taxa from the greenhouse
561 environment onto tomato plants (Supplemental Figure S2), but these taxa do
562 not appear to be establishing themselves on the plants and displacing
563 resident microbes. Taken together, we conclude that dispersal was present
564 in our system but not sufficient to explain the patterns we observe.
565 Importantly, the key findings that microbiomes vary amongst genotypes in
566 P1 and P2, and that the communities are well adapted to their environment
567 after four passages, are robust to the low-levels of dispersal that are likely to
568 have occurred. Future experiments should include filter traps or ”fake
569 plants” in order to explicitly test the prevalence and importance of dispersal
570 in the system. Such controls could also be used to measure the role of
571 ecological drift in shaping a community over time, independent of the host.
572 To directly test the alternative hypothesis that community changes
573 were due to neutral processes such as bottlenecking, ecological drift, or
574 random dispersal as discussed above, we first fit our data to neutral and null
575 models, finding a poorer fit over time. We next experimentally tested for

non-neutral microbiome adaption by conducting a community coalescence experiment to measure fitness of passaged microbiomes as compared to those from the start of the experiment. The results of this experiment strongly support the idea that these phyllosphere microbiomes adapted to the plant host environment over the course of four passages (Figure 4). Independent of overall bacterial abundance, P4 microbiomes were able to outcompete the less-adapted P1 microbiomes. One potential explanation for this ability of P4 communities to outcompete P1 is that the taxa that do particularly well in this environment, and are able to reach higher abundances at the end of P4, outcompete the taxa from P1 because they are at higher densities in the mixed inoculum. However, it is not clear how these possible density effects could be distinguished from the possibility that they are better adapted to the environment. Future work focusing on bacterial functional traits and/or culture-based experiments in which taxa are applied in different relative abundances could help shed insight to whether the observed competitive interactions were the result of density-dependent effects or competition.

The community coalescence approach [27] allowed us to demonstrate non-neutral selection of a bacterial community that is independent of host genotype and resistant to invasion by a more diverse, non-selected community. This approach was used by others in a study conducted on methanogenic bacterial communities [44]. The authors found that when multiple methanogenic communities were combined, a single

dominant community emerged from the mix. This emergent dominant community resembled the single community with the highest methane production that went into the combination, suggesting that the most-fit community is capable of reassembly, even in the presence of other community members.

While adaptation to both the local host environment (tomato plants, host genotype) and the larger environment (the greenhouse) were likely driving the increasingly non-neutral selection over time, the strength of within microbiome biotic interactions likely also increased over the course of the experiment. We see evidence for this through both increasing positive and negative community cohesion values. We also uncovered a strong effect of a greenhouse-acquired taxon on the community in one of the experiments (Figure S6). Though we are not able to determine what drove certain plants to be more colonized by this taxon than others, we did observe strong shifts in community composition associated with its relative abundance that may be due to spatial organization of plants in the greenhouse and/or stochastic initial colonization events. In a greenhouse study conducted on *Arabidopsis thaliana* phyllosphere communities, the authors found that abundance of certain dominant taxa could be tied to spatial organization of the plants that was likely driven by early stochastic events [15].

Although we focus primarily on the bacterial portion of the microbiome, the mycobiome changed over the course of passaging as well (Figure S7). Similar to the bacterial community, we observe significant decrease in

622 diversity and richness from P1 to P4, and we also see changing community
623 composition. We did not observe any effect of genotype on the fungal
624 community, but the low richness of fungi we recovered from leaf surfaces
625 may have impeded our ability to detect genotype-driven differences. It may
626 be the case that the dominant fungal taxa analyzed (epiphytic yeasts) were
627 not impacted by host genotype. Previous work that demonstrates plant
628 genotype influences the fungal community has primarily included
629 endophytes in addition to epiphytes in their collection and analysis [45–47].
630 The overall low richness of fungi we uncovered may be attributed to our
631 experimental methods, particularly the process of collecting microbes via
632 sonication, which may have biased passaging towards bacterial taxa and
633 fungal epiphytes. Yeasts are thought to be the dominant epiphytical fungal
634 group in the phyllosphere [48], and indeed, we find yeast to be in the highest
635 relative abundance compared to filamentous fungi. Although it is possible
636 that multi-kingdom interactions played a role in shaping community
637 composition (as has been demonstrated in *A. thaliana [49]*), we were unable
638 to perform these analyses due to the relatively few number of fungal taxa
639 that our analyses included. Similarly, our passaging method (e.g. pelleting
640 and removing supernatant at each passage) would have selected against
641 any free viruses; bacteriophages, mycovirsues, or others. Thus any effect of
642 viruses on the microbiome were eliminated from this study, although we
643 previously found that bacteriophages are capable of altering both abundance
644 and composition in the tomato phyllosphere [50]. It is possible that within

645 microbiome interactions may be contributing to the parallel changes
646 observed over time in the passaged lines. For this reason, and because there
647 is increasing interest in taking a multi-kingdom approach to studying the
648 microbiome, future work should be designed in a way that enhances the
649 collection and analysis of the complete microbiome, although technical
650 limitations often hinder our ability to do so.
651 Given the naturally distinct spatial structure, ease of sampling, high
652 culturability, and demonstrated role in plant health [24, 51], the
653 phyllosphere microbiome is an ideal model for testing theories of niche
654 selection and microbiome adaptation, as we have done here. Through spray
655 inoculation, the environment can be evenly saturated with diverse inoculum,
656 and it is possible to sample the successfully colonized community its
657 entirety. Moreover, bacterial abundance and growth can be tracked using
658 ddPCR, and communities can be described using next generation
659 sequencing. We were able to use the phyllosphere model to not only select
660 upon entire host-associated microbial communities, but to then
661 experimentally test our hypotheses regarding microbiome adaption in
662 subsequent experiments. These results also underscore the need for proper
663 no-selection control lines in any study evolving microbiomes that confer a
664 particular host-level trait.
665 Through this work, we also shed light on a notable challenge in
666 microbiome research. One intriguing interpretation of our data is that when
667 describing the microbiome of an open environment, such as plant surfaces,

many of the taxa found there may be transient visitors. In the case of the phyllosphere, there are microbes on leaf surfaces that may have emigrated from air, soil, surrounding plants, or other non-plant habitats and do not necessarily represent an adapted community that is capable of growth and persistence. Passaging of microbiomes in the absence of specific trait-based selection, as we have done here, is a powerful way of differentiating those taxa that are, or can rapidly become, well adapted to the plant host environment. It also raises the question as to if a microbiome should be defined as the community that is found upon sampling and sequencing, or if a true microbiome is one that is adapted to its host or environment.

Overall, we were able to show robust habitat selection of these communities over relatively short plant-host time scales. The results uncover great promise of this approach and system for answering fundamental questions about the forces shaping microbiome assembly over time, and also pave the way for selecting stable, uninvadable host-associated microbiomes, which may inform rational microbiome manipulation and probiotic design. Experiments such as these are crucial if we are to understand general principles governing microbiome assembly and adaptation and use this knowledge for transformative applications in both medicine and agriculture.

Materials/Methods (See supplement for complete methods)

Tomato accessions: Tomato accessions were obtained from the Tomato

Genetics Resource Center. Five tomato genotypes were used: *Solanum lycopersicum* money maker disease susceptible (TGRC 2706); *S. lycopersicum* money maker disease resistant (TGRC 3472); *S. lycopersicum* Rio Grande disease susceptible control for TGRC 3342 (TGRC 3343); *S. lycopersicum* Rio Grande disease resistant (TGRC 3342); and *S. pimpinellifolium* wild ancestor (2934). All genotypes were used for passages one, two, three, and p4-combined. Genotype 2934 was not used in passage four, as that genotype succumbed to fungal disease in the third generation. The community coalescence competition experiment included genotypes 2706, 3472, and 2934.

Tomato germination and growth: Seeds were surface sterilized using TGRC recommendations then transferred onto 1% water agar plates and placed in the dark at 21°C until emergence of the hypocotyl. At that point, seedling plates were moved into a growth chamber and allowed to continue germination for 1 week. After approximately one week, seedlings were transferred planted in sunshine mix #1 soil in seedling trays. After approximately one more week of growth, seedlings were transplanted into 8” diameter pots, making the plants approximately 2.5-3 weeks old at the first time of microbial inoculation. Age of inoculation varied slightly from experiment to experiment but was kept identical amongst genotypes within an experiment.

Inoculation preparation, first passage: Microbial inoculum for the first passage of the experiment was generated from field-grown tomato plants

from the UC Davis Student Organic Farm collected in September and October of 2016. Above-ground plant material was collected from various genotypes of tomatoes across nine different sites spread through four fields. Other plant types, such as lettuce, eggplant, corn, and oak trees, surrounded the tomato fields. Sterile phosphate freezing buffer was added to the bags of leaves, and the entire bags were placed in a Branson M5800 sonicating water bath. Material was sonicated for 10 minutes. This gentle sonication washes microbes from the surfaces of the leaves but does not damage cells. The resulting leaf wash from each site was pooled and divided into 6 aliquots and stored in glycerol freezing buffer. For each inoculation in the first passage, an aliquot was thawed, cells pelleted, and re-suspended in 200mL 10mM $MgCl_2$ buffer. Of this, 40mL were heat killed in an autoclave for a 30 minutes at 121°C. Both live and heat-killed inoculum were plated. There was no growth from heat-killed inoculum, and live-inoculum concentration was calculated to be 1.1 X 10 ^6 CFU/mL. Soil from each site, which had been stored at -20°C, was combined in a sterile bucket and thoroughly mixed before inoculation.

Inoculation procedure: Soil inoculation: The top layer of every pot was supplemented with 40 grams of UC Davis Farm Soil. Soil inoculation was only performed once and only for the first passage of plants. Spray inoculation: Each plant was sprayed with 4.5mL of inocula using misting spray tops. Control plants from passage 1 were inoculated with the heat-killed inocula. Control plants from P2 onward were inoculated with sterile

10mM $MgCl_2$. Immediately after inoculation, plants were placed in a random order in a high-humidity misting chamber for 24 hours. After 24 hours, the plants were moved to a greenhouse bench. Plants were inoculated once per week in the same manner and were placed in the misting chamber for 24 hours after every inoculation.

Plant sampling and inoculation preparation for passaging lines: Ten days after the final spray inoculation, plants were sampled. With the exception of the P4-Combined experiment, all plants were cut off at the base and immediately placed into sterile 1L bottles individually. By the end of P4-Combined, the plants had grown too large to sample the entire plant, and instead, roughly 2/3 of the plant material was sampled from each plant, with care taken to sample the same age of branches from every plant. After collection, plant material was weighed, sterile buffer added, and the entire bottle sonicated as above. Half of the volume from each plant was pelleted and re-suspended in ~1mL of 1:1 KB Broth Glycerol and stored at -80°C for inoculation of the subsequent passage. The other half of the volume was pelleted and stored as a pellet at -20°C for DNA extractions. To prepare inoculation of the next passage, microbiome glycerol stocks were thawed, briefly pelleted to remove glycerol, and re-suspended in sterile 10mM $MgCl_2$.

Inoculation preparation, combination of P4 microbiomes (Figure S7): Frozen microbiomes from all plants from the end of passage four were thawed, and half the volume was removed from each aliquot. These

aliquots were combined into one pooled meta-inoculum. This was divided into six aliquots. One was used immediately, and the rest of the aliquots were stored at -20°C in KB Glycerol and thawed by aliquot for each week of inoculation, as above.

P1, P4 coalescence experiment (Figure 5): Genotypes 2706, 3472, and 2934 were used for this experiment, and four plants of each genotype received each treatment (P1, P4, and Mix). One control plant of each genotype was spray inoculated with $MgCl_2$ as a control. To prepare the inoculum, microbiomes from the end of passage one and the end of passage four were combined. The same was done for all of the individual microbiomes that came off of passage 4 plants. In order to quantify only live cells, we used PMA treatment, using a method adapted from others [52], prior to ddPCR quantification (see below). Bacterial concentration was matched to 7.7×10^6 cells/mL. Plants were inoculated for three weeks and harvested 10 days after the final inoculation as described previously.

Bacterial quantification using ddPCR: The BioRad QX200 system was used for culture independent quantification of bacteria. Complete ddPCR methods are described elsewhere [50]. Bacterial abundance was measured directly after microbes were sonicated off plant surfaces into sterile buffer. For consistency, the same region of the 16S gene used below for amplicon sequencing was used for bacterial quantification. PNAs were used as well to limit any background amplification of plant mitochondrial or chloroplast DNA. All data were normalized to weight, in grams, and concentrations are

reported as 16S copy number/gram.

DNA extractions: DNA was extracted from microbial pellets using the Qiagen PowerSoil DNA extraction kit. A buffer control extraction was included for every set of extractions in order to identify and exclude taxa present in the dataset due to buffer contamination.

16S Libraries: The 16S rRNA gene was amplified using dual-indexed primers designed for the V3- V4 region [53] using the following primers: 341F (5 -CCTACGGGNBGCASCAG-3) and 785R (5 -GACTACNVGGGTATCTAATCC-3) [54]. Additionally, we also used peptide nucleic acids, PNAs [55] to decrease amplification of plant mitochondrial and chloroplast DNA. Negative buffer controls and PCR controls were sequenced along with experimental samples. Amplicons from each sample were pooled in equimolar concentrations, cleaned using an AMpure bead clean-up kit. Libraries were prepared for paired 300-PE reads in Illumina's MiSeq V3 platform (Illumina) at The California Institute for Quantitative Biosciences (QB3) at UC Berkeley.

ITS Libraries: Using the same DNA as above, the ITS2 region was amplified using ITS9-F: GAACGCAGCRAAIIGYGA and ITS4-R: TCCTCCGCTTATTGATATGC following a protocol published online by the Joint Genome Institute. A second PCR was performed (7 cycles) in order to anneal MiSeq illumunia adapters and barcodes onto the amplicons. PCRs were carried out in duplicate and pooled before they were prepared for sequencing by the QB3 sequencing facility as described above.

Sequence Processing and Data Analysis: MiSeq sequencing files were

demultiplexed by QB3 sequencing facility. Bacterial reads were combined into contigs using VSearch [56], and the remainder of the analysis was carried out in Mothur [57] following their MiSeq SOP [58] (See supplement for specifics). We used a 97% similarity cut-off for defining OTUs and the Silva reference database [59] for taxonomic assignment. Bacterial were rarified to 8,000 reads per sample. For the fungal community, an OTU table was generated from the fungal community sequencing data using QIIME2 (version 2018.8) (See supplement for specifics). Reads were clustered into OTUs at 97% identity and assigned taxonomy using the UNITE database and the feature-classifier plug-in [60]. Once bacterial and fungal OTU tables were generated in Mothur and QIIME2, the remainder of the analysis was performed in R using the following packages: Phyloseq [61], vegan [28], ampvis2 [62], and MicrobiomeSeq (Alfred Ssekagiri, William T. Sloan, Umer Zeeshan Ijaz). Occupancy-Abundance curves were generated using "Trifolium nodule microbiome analysis script" [63].

Incorporation of repeated measures into statistical models: In the serial passaging experiment, each microbiome line was independently passaged across four cohorts of tomato plants, and each microbiome line was sampled at the end of each passage. Although the microbiomes were never sampled multiple times from the same tomato plant, the data structure is similar to what one would find in time series experiment. Thus, wherever possible, "Line ID" was incorporated into models to take this into account. The following linear mixed effects model was utilized for

determining significant changes in diversity over time: lmer(Values ~ Passage + (1|LineID). In the case of PERMANOVAs, the strata term was used to limit permutations within Line IDs to test for the main effect of “Passage”. Furthermore, “Strata” cannot be utilized when determining significance of terms by=”margin” (Type III tests). Instead, significance is assigned to each term sequentially from first to last. Thus, order of terms in the model may impact significance. In the data presented in this manuscript, all iterations of term order were tested in each model. Statistics are presented using the following models with the use of strata: adonis(bray.matrix ~ Passage + Genotype, permutations=999, strata= LineID). Importantly, although changing the order of terms sometimes slightly altered the R^2 values, none of the differences had any impact on a variable’s significance level. Changing the order of terms did not impact the interpretation of the importance of any variable tested in this dataset. The adonis2 test with the by=”margin” term was used whenever the strata term was not included in the model. The following model was utilized in these cases: adonis(bray.matrix ~ Passage + SampleType, method=”bray”, by=”margin”, permutations=999).

Community Cohesion Metrics: The estimations of positive and negative cohesion values follows the cohesion metrics approach proposed by Herren *et al*. [37]. We modified their method to estimate cohesion values by using two relative abundance profiles of a training set and test set. Relative abundance profile of the training set was obtained by randomly selecting half of the samples in each microbiome passage. The test set consists of the

other half of the samples. Using the training set and following the same procedure as Herren *et al*., connectedness metrics were calculated. The estimated connectedness metrics subtracts a null model. The obtained connectedness metrics are multiplied by relative abundance profile of test set to estimate positive and negative cohesion values. Two hundred iterations of sampling randomization in each microbiome passage were carried out at OTU level to obtain training set and test set for P1, P2, P3, and P4.

Neutral model: The neutral model was proposed by Sloan *et al*. to describe both microbial diversity and taxa-abundance distribution of a community [41]. Burns *et al*. [18] have developed a R package based on Sloan's neutral model to determine the importance of neutral processes to community assembly. In brief, the neutral model creates a potential neutral community by a single free parameter describing the migration rate, *m*, based on two sets of abundance profiles – a local community and metacommunities. The local community describes the observed relative abundance of OTUs, while the metacommunity is estimated by the mean relative abundance across all local communities. The estimated migration rate is the probability of OTU dispersal from the metacommunity to replace a randomly lost individual in the local community. The migration rate can be interpreted as dispersal limitation. In each microbiome passage, half of the samples were randomly selected and the relative abundance profile at the OTU level was used. The neutral model fit and migration rate were estimated in the resolution results

of 200 iterations for P1, P2, P3, P4, and P4 Combined.

Null model predictions: We applied a null model approach on the serial passaging data P1-P4 to characterize the changes of stochastic process driving the assembly of plant microbiome over time. Lines that had high quality sequencing data at every time point (thirteen in total) were used for this analysis. The null scenario for each line at each passage was generated using the data for that same line at the previous passage. The null scenario of P1 was generated using the original field inoculum sample. The null model approach was based on community pairwise dissimilarity proposed by Chase and Myers [64] and extended by Stegen *et al.* to incorporate species abundance [65]. Chase and Myers proposed a degree of species turnover by a randomization procedure where species probabilistically occur at each local community until observed local richness is reached. However, the estimated degree of turnover does not include species abundance. To take full advantage of our dataset, we also incorporated species relative abundance into the procedure proposed by Stegen *et al*. Zinger *et al*. has developed R code for the null model and applied the null model approach on the soil microbiome [38]. This approach does not require *a priori* knowledge of the local community condition and determines if each plant microbiome at the current passage deviates from a null scenario generated by that same microbiome at the previous passage. In brief, the null scenario of each was generated by random resampling of OTUs and remained the same richness and number of reads with the original sample. Total OTUs observed in the

sample and the corresponding relative abundance was used as probabilities of selecting an OTU and its associated number of reads, respectively. The Bray-Curtis metric is used to calculate dissimilarities across null communities with 1,000 permutations. The average of dissimilarities among permutations represents null expectations of community dissimilarities. The null deviation shows the differences between average null expectation and the observed microbiome of the same line.

Acknowledgements

The authors would like to acknowledge the UC Davis Student Farm, who provided access to the fields from which the original inoculum was generated. They would also like to thank Christina Winstrom and the Oxford Tract greenhouse staff for their role in plant care throughout the experiments. The authors thank Shirley Zhang for assistance with plant inoculation. The authors thank members of the Coleman-Derr lab at UC Berkeley for their helpful input on analysis of these data. Lastly, the authors thank Dylan Smith and Shana McDevitt for their continued support with sequencing efforts for the experiment. We'd like to acknowledge Academia Sinica, Taiwan and the affiliated faculty Dr. Daryi Wang, which provided the International Research Short-term Visiting Scholarship Fund for Francis Weng to conduct research at University of California, Berkeley. The work was supported by the National Science Foundation (NSF DEB 1754494).

References

1. Gopal M, Gupta A (2016) Microbiome Selection Could Spur Next-Generation Plant Breeding Strategies. Front Microbiol 7:. https://doi.org/10.3389/fmicb.2016.01971

2. Orozco-Mosqueda M del C, Rocha-Granados M del C, Glick BR, Santoyo G (2018) Microbiome engineering to improve biocontrol and plant growth-promoting mechanisms. Microbiol Res 208:25–31. https://doi.org/10.1016/j.micres.2018.01.005

3. Mimee M, Citorik RJ, Lu TK (2016) Microbiome Therapeutics – Advances and Challenges. Adv Drug Deliv Rev 105:44–54. https://doi.org/10.1016/j.addr.2016.04.032

4. Panke-Buisse K, Poole AC, Goodrich JK, et al (2015) Selection on soil microbiomes reveals reproducible impacts on plant function. ISME J 9:980–989. https://doi.org/10.1038/ismej.2014.196

5. Marasco R, Rolli E, Ettoumi B, et al (2012) A drought resistance-promoting microbiome is selected by root system under desert farming. PloS One 7:e48479. https://doi.org/10.1371/journal.pone.0048479

6. Rolli E, Marasco R, Vigani G, et al (2015) Improved plant resistance to drought is promoted by the root-associated microbiome as a water stress-dependent trait. Environ Microbiol 17:316–331. https://doi.org/10.1111/1462-2920.12439

7. Fitzpatrick CR, Mustafa Z, Viliunas J (2019) Soil microbes alter plant fitness under competition and drought. J Evol Biol 32:438–450. https://doi.org/10.1111/jeb.13426

8. Pineda A, Kaplan I, Bezemer TM (2017) Steering Soil Microbiomes to Suppress Aboveground Insect Pests. Trends Plant Sci 22:770–778. https://doi.org/10.1016/j.tplants.2017.07.002

9. Wagner MR, Lundberg DS, del Rio TG, et al (2016) Host genotype and age shape the leaf and root microbiomes of a wild perennial plant. Nat Commun 7:12151. https://doi.org/10.1038/ncomms12151

10. Bodenhausen N, Bortfeld-Miller M, Ackermann M, Vorholt JA (2014) A Synthetic Community Approach Reveals Plant Genotypes Affecting the Phyllosphere Microbiota. PLOS Genet 10:e1004283. https://doi.org/10.1371/journal.pgen.1004283

11. Costello EK, Lauber CL, Hamady M, et al (2009) Bacterial Community Variation in Human Body Habitats Across Space and Time. Science 326:1694–1697. https://doi.org/10.1126/science.1177486

12. Benson AK, Kelly SA, Legge R, et al (2010) Individuality in gut microbiota composition is a complex polygenic trait shaped by multiple environmental and host genetic factors. Proc Natl Acad Sci U S A 107:18933–18938. https://doi.org/10.1073/pnas.1007028107

13. Spor A, Koren O, Ley R (2011) Unravelling the effects of the environment and host genotype on the gut microbiome. Nat Rev Microbiol 9:279–290. https://doi.org/10.1038/nrmicro2540

14. Micallef SA, Channer S, Shiaris MP, Colón-Carmona A (2009) Plant age and genotype impact the progression of bacterial community succession in the Arabidopsis rhizosphere. Plant Signal Behav 4:777–780. https://doi.org/10.4161/psb.4.8.9229

15. Maignien L, DeForce EA, Chafee ME, et al (2014) Ecological Succession and Stochastic Variation in the Assembly of Arabidopsis thaliana Phyllosphere Communities. Mbio 5:e00682-13. https://doi.org/10.1128/mBio.00682-13

16. Rothschild D, Weissbrod O, Barkan E, et al (2018) Environment dominates over host genetics in shaping human gut microbiota. Nature 555:210–215. https://doi.org/10.1038/nature25973

17. Laforest-Lapointe I, Messier C, Kembel SW (2016) Host species identity, site and time drive temperate tree phyllosphere bacterial community structure. Microbiome 4:27. https://doi.org/10.1186/s40168-016-0174-1

18. Burns AR, Miller E, Agarwal M, et al (2017) Interhost dispersal alters microbiome assembly and can overwhelm host innate immunity in an experimental zebrafish model. Proc Natl Acad Sci 114:11181–11186. https://doi.org/10.1073/pnas.1702511114

19. Ebert D (1998) Experimental evolution of parasites. Science 282:1432–1435

20. Buckling A, Craig Maclean R, Brockhurst MA, Colegrave N (2009) The Beagle in a bottle. Nature 457:824–829. https://doi.org/10.1038/nature07892

21. MORRIS CE (2002) Fifty years of phyllosphere microbiology : significant contributions to research in related fields. Phyllosphere Microbiol

22. Berg M, Koskella B (2018) Nutrient-and Dose-Dependent Microbiome-Mediated Protection against a Plant Pathogen. Curr Biol

23. Innerebner G, Knief C, Vorholt JA (2011) Protection of Arabidopsis thaliana against leaf-pathogenic Pseudomonas syringae by Sphingomonas strains in a controlled model system. Appl Environ Microbiol 77:3202–3210. https://doi.org/10.1128/AEM.00133-11

24. Fürnkranz M, Wanek W, Richter A, et al (2008) Nitrogen fixation by phyllosphere bacteria associated with higher plants and their colonizing epiphytes of a tropical lowland rainforest of Costa Rica. ISME J 2:561–570. https://doi.org/10.1038/ismej.2008.14

25. Stone BWG, Weingarten EA, Jackson CR (2018) The Role of the Phyllosphere Microbiome in Plant Health and Function. In: Annual Plant Reviews online. American Cancer Society, pp 1–24

26. Williams TR, Marco ML (2014) Phyllosphere Microbiota Composition and Microbial Community Transplantation on Lettuce Plants Grown Indoors. mBio 5:e01564-14. https://doi.org/10.1128/mBio.01564-14

27. Rillig MC, Antonovics J, Caruso T, et al (2015) Interchange of entire communities: microbial community coalescence. Trends Ecol Evol 30:470–476. https://doi.org/10.1016/j.tree.2015.06.004

28. Dixon P, Palmer MW (2003) VEGAN, a package of R functions for community ecology. J Veg Sci 14:927–930. https://doi.org/10.1658/1100-9233(2003)014[0927:VAPORF]2.0.CO;2

29. Anderson MJ (2001) A new method for non-parametric multivariate analysis of variance: NON-PARAMETRIC MANOVA FOR ECOLOGY. Austral Ecol 26:32–46. https://doi.org/10.1111/j.1442-9993.2001.01070.pp.x

30. Anderson MJ (2006) Distance-based tests for homogeneity of multivariate dispersions. Biometrics 62:245–253. https://doi.org/10.1111/j.1541-0420.2005.00440.x

31. Anderson MJ, Ellingsen KE, McArdle BH (2006) Multivariate dispersion as a measure of beta diversity. Ecol Lett 9:683–693. https://doi.org/10.1111/j.1461-0248.2006.00926.x

32. Segata N, Izard J, Waldron L, et al (2011) Metagenomic biomarker discovery and explanation. Genome Biol 12:R60. https://doi.org/10.1186/gb-2011-12-6-r60

33. Klappenbach JA, Dunbar JM, Schmidt TM (2000) rRNA operon copy number reflects ecological strategies of bacteria. Appl Environ Microbiol 66:1328–1333. https://doi.org/10.1128/aem.66.4.1328-1333.2000

34. Roller BRK, Stoddard SF, Schmidt TM (2016) Exploiting rRNA Operon Copy Number to Investigate Bacterial Reproductive Strategies. Nat Microbiol 1:16160. https://doi.org/10.1038/nmicrobiol.2016.160

35. Shrestha PM, Noll M, Liesack W (2007) Phylogenetic identity, growth-response time and rRNA operon copy number of soil bacteria indicate different stages of community succession. Environ Microbiol 9:2464–2474. https://doi.org/10.1111/j.1462-2920.2007.01364.x

36. Stoddard SF, Smith BJ, Hein R, et al (2015) rrnDB: improved tools for interpreting rRNA gene abundance in bacteria and archaea and a new foundation for future development. Nucleic Acids Res 43:D593-598. https://doi.org/10.1093/nar/gku1201

37. Herren CM, McMahon KD (2017) Cohesion: a method for quantifying the connectivity of microbial communities. ISME J 11:2426–2438. https://doi.org/10.1038/ismej.2017.91

38. Zinger L, Taberlet P, Schimann H, et al (2019) Body size determines soil community assembly in a tropical forest. Mol Ecol 28:528–543. https://doi.org/10.1111/mec.14919

39. Wright DH (1991) Correlations Between Incidence and Abundance are Expected by Chance. J Biogeogr 18:463–466. https://doi.org/10.2307/2845487

40. Gonzalez A, Lawton JH, Gilbert FS, et al (1998) Metapopulation Dynamics, Abundance, and Distribution in a Microecosystem. Science 281:2045–2047. https://doi.org/10.1126/science.281.5385.2045

41. Sloan WT, Woodcock S, Lunn M, et al (2007) Modeling Taxa-Abundance Distributions in Microbial Communities using Environmental Sequence Data. Microb Ecol 53:443–455. https://doi.org/10.1007/s00248-006-9141-x

42. Gould AL, Zhang V, Lamberti L, et al (2018) Microbiome interactions shape host fitness. Proc Natl Acad Sci 115:E11951–E11960. https://doi.org/10.1073/pnas.1809349115

43. Lymperopoulou DS, Adams RI, Lindow SE (2016) Contribution of vegetation to the microbial composition of nearby outdoor air. Appl Environ Microbiol AEM.00610-16. https://doi.org/10.1128/AEM.00610-16

44. Sierocinski P, Milferstedt K, Bayer F, et al (2017) A Single Community Dominates Structure and Function of a Mixture of Multiple Methanogenic Communities. Curr Biol 27:3390-3395.e4. https://doi.org/10.1016/j.cub.2017.09.056

45. Qian X, Duan T, Sun X, et al (2018) Host genotype strongly influences phyllosphere fungal communities associated with Mussaenda pubescens var. alba (Rubiaceae). Fungal Ecol 36:141–151. https://doi.org/10.1016/j.funeco.2018.10.001

46. Sapkota R, Knorr K, Jorgensen LN, et al (2015) Host genotype is an important determinant of the cereal phyllosphere mycobiome. New Phytol 207:1134–1144. https://doi.org/10.1111/nph.13418

47. Bálint M, Tiffin P, Hallström B, et al (2013) Host Genotype Shapes the Foliar Fungal Microbiome of Balsam Poplar (Populus balsamifera). PLoS ONE 8:. https://doi.org/10.1371/journal.pone.0053987

48. Whipps JM, Hand P, Pink D, Bending GD (2008) Phyllosphere microbiology with special reference to diversity and plant genotype. J Appl Microbiol 105:1744–1755. https://doi.org/10.1111/j.1365-2672.2008.03906.x

49. Agler MT, Ruhe J, Kroll S, et al (2016) Microbial Hub Taxa Link Host and Abiotic Factors to Plant Microbiome Variation. PLOS Biol 14:e1002352. https://doi.org/10.1371/journal.pbio.1002352

50. Morella NM, Gomez AL, Wang G, et al (2018) The impact of bacteriophages on phyllosphere bacterial abundance and composition. Mol Ecol. https://doi.org/10.1111/mec.14542

51. Elbeltagy A, Nishioka K, Sato T, et al (2001) Endophytic Colonization and In Planta Nitrogen Fixation by a Herbaspirillum sp. Isolated from Wild Rice Species. Appl Env Microbiol 67:5285–5293. https://doi.org/10.1128/AEM.67.11.5285-5293.2001

52. Carini P, Marsden PJ, Leff JW, et al (2017) Relic DNA is abundant in soil and obscures estimates of soil microbial diversity. Nat Microbiol 2:16242. https://doi.org/10.1038/nmicrobiol.2016.242

53. Naylor D, DeGraaf S, Purdom E, Coleman-Derr D (2017) Drought and host selection influence bacterial community dynamics in the grass root microbiome. ISME J 11:2691. https://doi.org/10.1038/ismej.2017.118

54. Takahashi S, Tomita J, Nishioka K, et al (2014) Development of a Prokaryotic Universal Primer for Simultaneous Analysis of Bacteria and Archaea Using Next-Generation Sequencing. PLOS ONE 9:e105592. https://doi.org/10.1371/journal.pone.0105592

55. Lundberg DS, Yourstone S, Mieczkowski P, et al (2013) Practical innovations for high-throughput amplicon sequencing. Nat Methods 10:999–1002. https://doi.org/10.1038/nmeth.2634

56. Rognes T, Flouri T, Nichols B, et al (2016) VSEARCH: a versatile open source tool for metagenomics. PeerJ Preprints

57. Schloss PD, Westcott SL, Ryabin T, et al (2009) Introducing mothur: open-source, platform-independent, community-supported software for describing and comparing microbial communities. Appl Environ Microbiol 75:7537–7541. https://doi.org/10.1128/AEM.01541-09

58. Kozich JJ, Westcott SL, Baxter NT, et al (2013) Development of a dual-index sequencing strategy and curation pipeline for analyzing amplicon sequence data on the MiSeq Illumina sequencing platform. Appl Environ Microbiol 79:5112–5120. https://doi.org/10.1128/AEM.01043-13

59. Quast C, Pruesse E, Yilmaz P, et al (2013) The SILVA ribosomal RNA gene database project: improved data processing and web-based tools. Nucleic Acids Res 41:D590–D596. https://doi.org/10.1093/nar/gks1219

60. Bokulich NA, Kaehler BD, Rideout JR, et al (2018) Optimizing taxonomic classification of marker-gene amplicon sequences with QIIME 2's q2-feature-classifier plugin. Microbiome 6:90. https://doi.org/10.1186/s40168-018-0470-z

61. McMurdie PJ, Holmes S (2013) phyloseq: An R Package for Reproducible Interactive Analysis and Graphics of Microbiome Census Data. PLOS ONE 8:e61217. https://doi.org/10.1371/journal.pone.0061217

62. Skytte Andersen KS, Kirkegaard RH, Karst SM, Albertsen M (2018) ampvis2: an R package to analyse and visualise 16S rRNA amplicon data. bioRxiv 299537. https://doi.org/10.1101/299537

63. Trifolium nodule microbiome analysis script

64. Chase JM, Myers JA (2011) Disentangling the importance of ecological niches from stochastic processes across scales. Philos Trans R Soc Lond B Biol Sci 366:2351–2363. https://doi.org/10.1098/rstb.2011.0063

65. Stegen JC, Lin X, Fredrickson JK, et al (2013) Quantifying community assembly processes and identifying features that impose them. ISME J 7:2069–2079. https://doi.org/10.1038/ismej.2013.93

Figure Legends

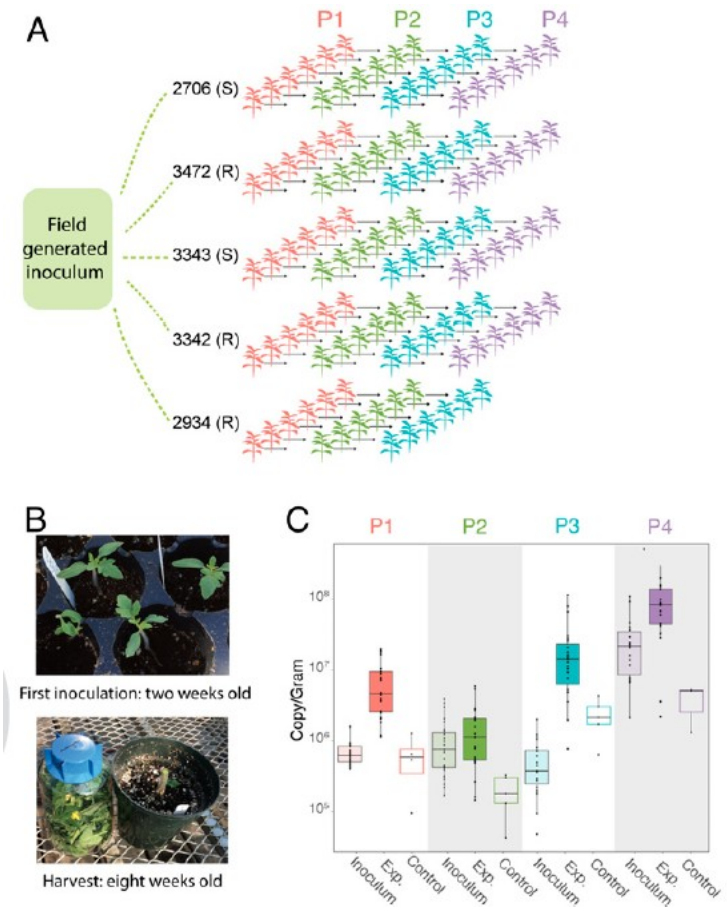

Figure 1 Serial passaging of the phyllosphere microbiome

Experimental design of serial passaging experiment in which microbial inoculum from an agricultural tomato field was inoculated onto replicates of five genotypes and passaged for four passages (a). Plants were first

inoculated when they were 2 weeks old, and the entire plant was sampled at 8 weeks old (b). Bacterial abundance was measured at the end of each passage from experimental and control plants using ddPCR and normalized to the weight of each plant. Inoculum density was calculated as well (c). Note that our measures of bacterial growth likely overestimate the starting densities and do not account for population turnover (as a result of cell death and replacement within a passage), and are therefore highly conservative.

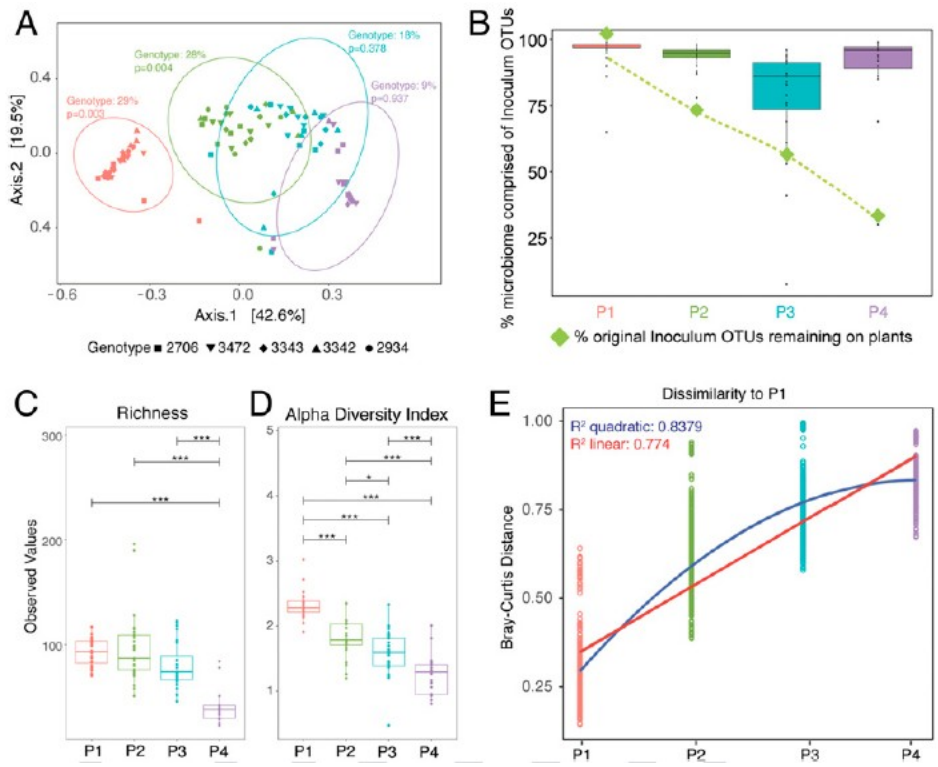

Figure 2 Bacterial community change over time

PCoA plots of Bray-Curtis dissimilarity show a significant effect (determined

by a PERMANOVA test) of genotype in P1 and P2 (a) Ellipses indicate 95% confidence around the clustering. The percent of original inoculum OTUs present at each passage was calculated (green diamonds), and the reads/sample of inoculum OTUs out of total reads was calculated for each plant at every passage and displayed on a box plot (b). Plots of richness (c) and Shannon's alpha diversity index (d) at each passage show a significant decrease over time. Bray-Curtis dissimilarities between microbiomes in P1 were compared to those in P1, P2, P3, and P4, and linear and quadratic models were fit to the data (e). Corrected p values of multiple pairwise comparisons in (c) and (d) are illustrated on the graph * p≤0.05; ** p≤0.01; *** p≤0.001; ****p≤0.0001.

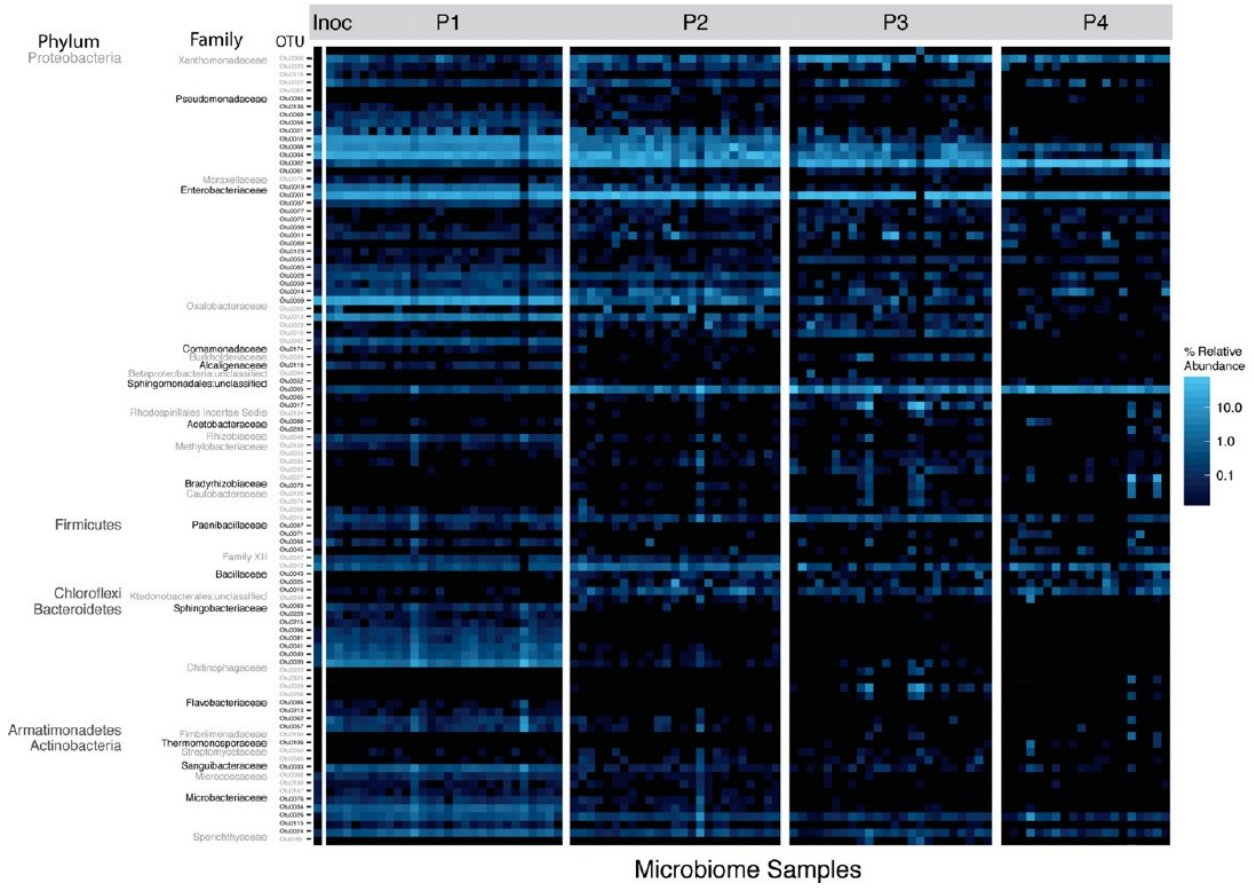

Figure 3 Changing relative abundance of top 100 OTUs

A heat map showing relative abundance of the top 100 OTUs illustrates the changing community composition at multiple taxonomic levels. Full taxonomy of OTUs is found in Supplemental Table 1.

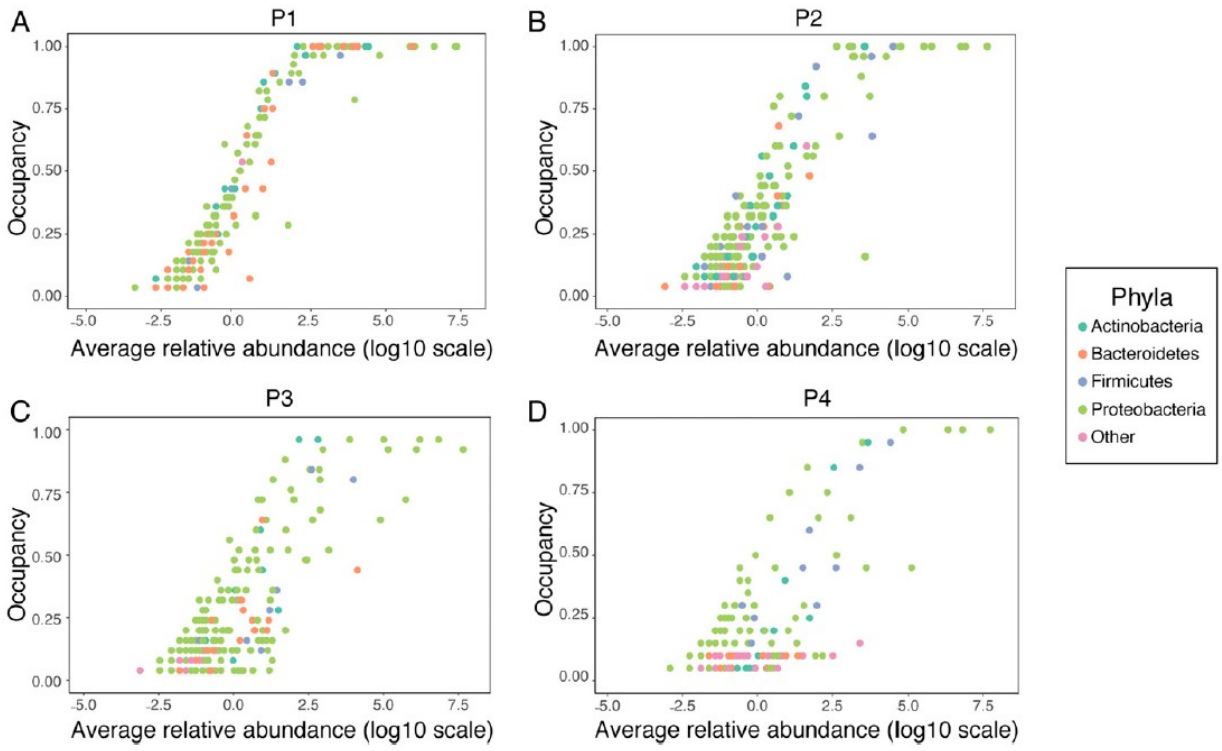

Figure 4 Occupancy- Abundance curves

For each OTU, its occupancy (or, proportion of plant hosts in which it was found) is plotted against the log (10) of its relative abundance. OTUs belonging to phyla other than those in the top four phyla are classified as "other".

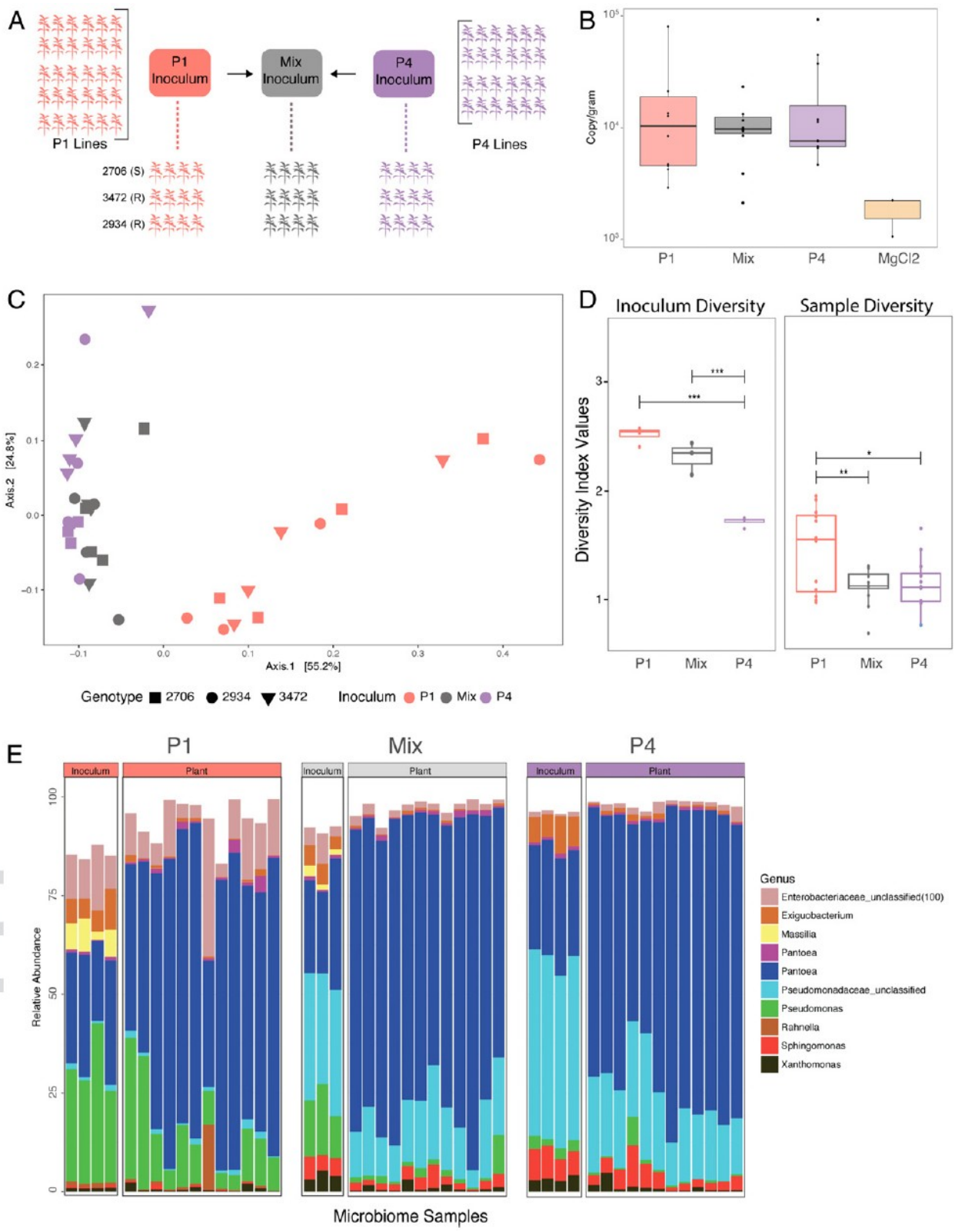
A
P1 Inoculum
Mix Inoculum
P4 Inoculum
P1 Lines
P4 Lines
2706 (S)
3472 (R)
2934 (R)
B
Copy/gram
P1
Mix
P4
MgCl2
C
Axis.2 [24.8%]
Axis.1 [55.2%]
Genotype 2706 2934 3472
Inoculum P1 Mix P4
D
Inoculum Diversity
Sample Diversity
Diversity Index Values
E
P1
Mix
P4
Inoculum
Plant
Relative Abundance
Microbiome Samples
Genus
Enterobacteriaceae_unclassified(100)
Exiguobacterium
Massilia
Pantoea
Pantoea
Pseudomonadaceae_unclassified
Pseudomonas
Rahnella
Sphingomonas
Xanthomonas

Figure 5 Testing microbiome adaptation

Plants were inoculated with pooled, passaged microbiomes from the end of P1, P4, or a 50:50 Mix of the two (a). Bacterial abundance was measured using ddPCR (b). A PCoA plot of Bray-Curtis dissimilarity (colored by inoculum source) shows that P1 plants have bacterial communities that are significantly different from P4 and Mix plants, which are indistinguishable (c). Shannon's alpha diversity index of the inoculum and experimental plants (d) show significant differences between samples. A bar graph illustrating composition of the top 10 OTUs shows differences in taxa amongst both the inoculum and experimental plants (e). Corrected p values of multiple pairwise comparisons in (d) are illustrated on the graph * $p \leq 0.05$; ** $p \leq 0.01$; *** $p \leq 0.001$; **** $p \leq 0.0001$.